

Article

Autonomous Hydrodistillation with a Digital Twin for Efficient and Climate Neutral Manufacturing of Phytochemicals

Alexander Uhl ¹, Larissa Knierim ¹, Theresa Höß ², Marcel Flemming ², Axel Schmidt ¹ and Jochen Strube ^{1,*}

¹ Institute for Separation and Process Technology, Clausthal University of Technology, Leibnizstr. 15, D38678 Clausthal-Zellerfeld, Germany

² SKH GmbH, Koenigbacher Strasse 17, D94496 Ortenburg, Germany

* Correspondence: strube@itv.tu-clausthal.de

Abstract: Hydrodistillation is traditionally a green technology for the manufacturing of natural products that are volatile. As well as acknowledged process intensification methods such as microwave support for energy efficiency to move towards climate neutral operation, digital twins combined with process analytical technology for advanced process control enables reliable operation of an optimal operation point regarding lowest cost of goods, as well as lowest global warming potential equivalent. A novel process control enabled by digital twin technology has shown to reduce the ecological footprint of the extraction by up to 46.5%, while reducing the cost of extraction by 22.4%. Additionally, skilled operator time is reduced, and the sustainable plant material is utilized most efficiently. The approach is ready to apply, but broad industrialization seems to be held back by unclear business cases and lack of comprehension of decision makers. This is in drastic contrast to the political demand for climate neutrality goals and the cost pressure by worldwide completion.

Keywords: green technology; hydrodistillation; phytochemicals; natural products; digital twin; autonomous operation; process analytical technology; sustainability; climate neutrality



Citation: Uhl, A.; Knierim, L.; Höß, T.; Flemming, M.; Schmidt, A.; Strube, J. Autonomous Hydrodistillation with a Digital Twin for Efficient and Climate Neutral Manufacturing of Phytochemicals. *Processes* **2024**, *12*, 217. <https://doi.org/10.3390/pr12010217>

Academic Editors: Jiaqiang E and Stefania Tronci

Received: 7 November 2023

Revised: 9 January 2024

Accepted: 15 January 2024

Published: 18 January 2024



Copyright: © 2024 by the authors. Licensee MDPI, Basel, Switzerland. This article is an open access article distributed under the terms and conditions of the Creative Commons Attribution (CC BY) license (<https://creativecommons.org/licenses/by/4.0/>).

1. Introduction

“Green extraction is based on the discovery and design of extraction processes which will reduce energy consumption, allows use of alternative solvents and renewable natural products, and ensure a safe and high quality extract/product.”—Farid Chemat [1].

Plant material is used in modern and ancient pharmaceutical and aromatic applications [2]. In comparison to synthesis, feedstock in phytochemicals has a lower carbon footprint and environmental impact [3–5]. Distillation processes for the recovery of volatile phytochemicals are divided into steam distillation and hydrodistillation and are by definition green extraction technologies. However, both process variants require energy for continuous evaporation of water. Given the definition of green extraction above, it is important to develop technologies and solutions for optimized, sustainable processes. Process intensification with microwave, ultrasonic sound and pulsed electric fields is one feasible approach [6]. In addition, digital twins on the basis of rigorous models enable the realization of reliable operation at optimized conditions, based on quantitative design and control strategies obtained and defined by Quality-by-Design (QbD) principles [7].

In order to meet targets of climate neutrality while still remaining economically sustainable, process efficiency is one of the most important factors to be worked on. This can be achieved by upgrading process equipment [8] or implementing efficient process control [9]. A novel approach to process control is model predictive control via digital twin (DT), which has improved process sustainability [10,11]. In previous studies it was found that this control can reduce global warming potential (GWP) and the production cost of plant extraction processes [12].

This work shows the reduction of environmental footprint and increased economic competitiveness enabled by digital twins technology for autonomous operation. This is

demonstrated by the example of fragrances as a typical application for hydrodistillation; however, the methodology can and has been transferred to other processes in chemical and pharmaceutical engineering.

1.1. Hydrodistillation

Distillation as a separation or extraction process was found for the first time 79 AD in the literature [13,14]. Distillation was described not only as the extraction of alcohols, but also as the extraction of oils from plant material. Continuous development of extraction equipment and separation of the subordinated processes took place, along with the increase in their economic and social relevance. In this process, equipment is developed from small glass apparatuses [15] to columns made of stainless steel for large-scale production and separation of liquids [16,17]. Rectification, steam distillation and hydrodistillation emerged from the superordinate distillation [18,19].

Distillation processes for the recovery of volatile phytochemicals are divided into steam distillation and hydrodistillation.

In steam distillation, the plant material is packed into the distillation column and then passed through by rising steam. Together with the steam, oil components from the plant material rise to the top of the column, are condensed and subsequently separate from the aqueous phase in the separator. In laboratory scale and according to Ph. Eur. a cleverger-type is used for condensation (see also Figure 1) [20–22].

Hydrodistillation is used if the plant material is present directly in the heated water vessel. The plant material is extracted by maceration, whereby the oil components evaporate together with the water and are then condensed and separated from the aqueous phase in the separator, as in the case of steam distillation [23]. The aqueous phase after condensation and phase separation may contain portions of oil in small amounts (<50 mg/L) and this is referred to as a hydrolate or hydrosol [24].

The recirculation of the aqueous hydrolate phase serves, on the one hand, to prevent the water reservoir from completely emptying through evaporation and can also serve to increase the yield of the process by recovering oil components in the hydrolate through renewed evaporation [25]. This process variant is called hydrodistillation with cohobation [26].

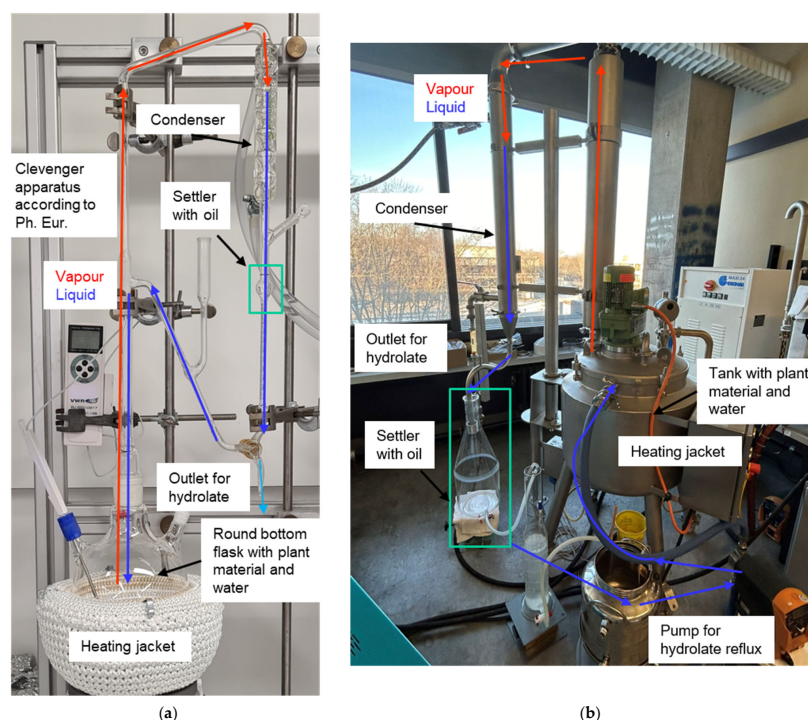


Figure 1. Laboratory distillation column (a) [27]; hydrodistillation pilot plant (b).

The content of long-chain fatty acids (e.g., myristic acid, etc.), determines the melting point and physical state of the organic extract. If the extract is liquid at room temperature, it is called oil or essential oil. The general monograph was adopted in a chapter dedicated to essential oils in the Ph. Eur. [28]. After hydrodistillation, the extract of iris rhizome is present in liquid form (oil) at temperatures above 45 °C. At room temperature, the oil solidifies. The solid thus obtained is called iris butter [29]. Analysis of the oil and hydrolate is usually performed by gas chromatography (GC) [30,31].

Steam distillation was used in the 10th century as a process for the extraction of rose water [32]. The vast majority of the models discussed in the literature, despite the long-standing, widespread application of these processes, are nevertheless comparatively simple and are mostly based on a first order kinetics approach [33–35].

These models usually do not separately account for the core phenomena that actually take place, such as the s/l extraction that initially takes place, the subsequent evaporation, the condensation, and the l/l phase separation.

A common core equation of such a kinetic model, often takes a form as shown in Equation (1).

$$\frac{q_0 - q}{q_0} = (1 - b) \times e^{-kt} \quad (1)$$

Here q_0 represents the initial loading of the plant material, q represents the current loading, and t represents the process time. b and k are effectively fit factors that are fitted to known process trajectories. It is obvious that such models cannot separately represent the different influences of fluid dynamics, phase equilibrium, or kinetics on the process outcome.

There is little work in the literature that links these individual elementary processes. Sovova and Aleksovski [36], for example, published a study in which different particle morphologies and the influence of the oil location on the extraction process were investigated in detail. However, the yield after subsequent distillation was just described on the basis of retrofitted profiles.

The vapor pressure of the mixture is one of the most important equilibrium parameters for predicting the distillation process. For steam distillation, it can be obtained from the Hausbrand diagram for different organic components and temperatures [37]. It represents the total vapor pressure of the mixture as the sum of the vapor pressures of the organic and aqueous phases. If the components are almost completely immiscible, this relationship simplifies to [38]:

$$P_{tot} = P_{0org} + P_{0w} = P_{org} + P_W \quad (2)$$

1.2. Process Analytical Technologies

In the application of Quality by Design-based process design, the development of a process analytical technologies (PAT) concept represents the interface between the digital twin and the process [39,40]. By means of PAT, critical process parameters can be measured and adjusted in combination with the digital twin within the framework of Advanced Process Control [41]. In this course, the process status and the further course of the extraction can also be predicted [41].

A challenge here is the choice of the spectroscopic measurement method. For example, DAD is suitable for the detection of small concentrations in solutions, whereas FTIR is better suited to differentiate between substances and substance groups [42].

Another point to consider when designing a PAT concept is the nature of the process and the parameters to be determined. For example, the corresponding probe can be installed directly in the process or a flow cell can be operated in a bypass. In the specific case of hydrodistillation, care must be taken to ensure that the oil remains liquid during measurement. This can be achieved with a temperature-controlled measuring cell, for example. When operating in the bypass, it is also necessary to determine the height of the phase interface so that the essential oil sample is not contaminated with aqueous hydrolate.

1.3. Digital Twin

Digital twins are based on validated, rigorous process models [43]. These, again, must be able to separately describe the different contributions of fluid dynamics, phase equilibrium, and mass transfer kinetics to the process outcome. They are available for all units used in common separation processes, such as SLE, LLE, membrane processes, precipitation, chromatography, and steam distillation. Distinct and quantitative validation criteria and workflows are available [39,44].

In addition to the process model, the development of a digital twin also requires PAT. PAT is used to make the necessary process information available to the process model online and in real time in order to make process predictions and, if necessary, to recognize changing optimal process conditions and to pass them on to the process control system [42]. Suitable PAT detectors and selection criteria for different processes have been described in many cases. The control of the process directly, the latter variant, shows that a digital twin requires not only the process information interface from the physical to the digital representation of the process, but also the interface from the digital back to the physical process. As for the demonstration of validated process models, the implementation and validation of digital twin technology has also been shown in a number of publications [12] and the general workflow is shown in Figure 2.

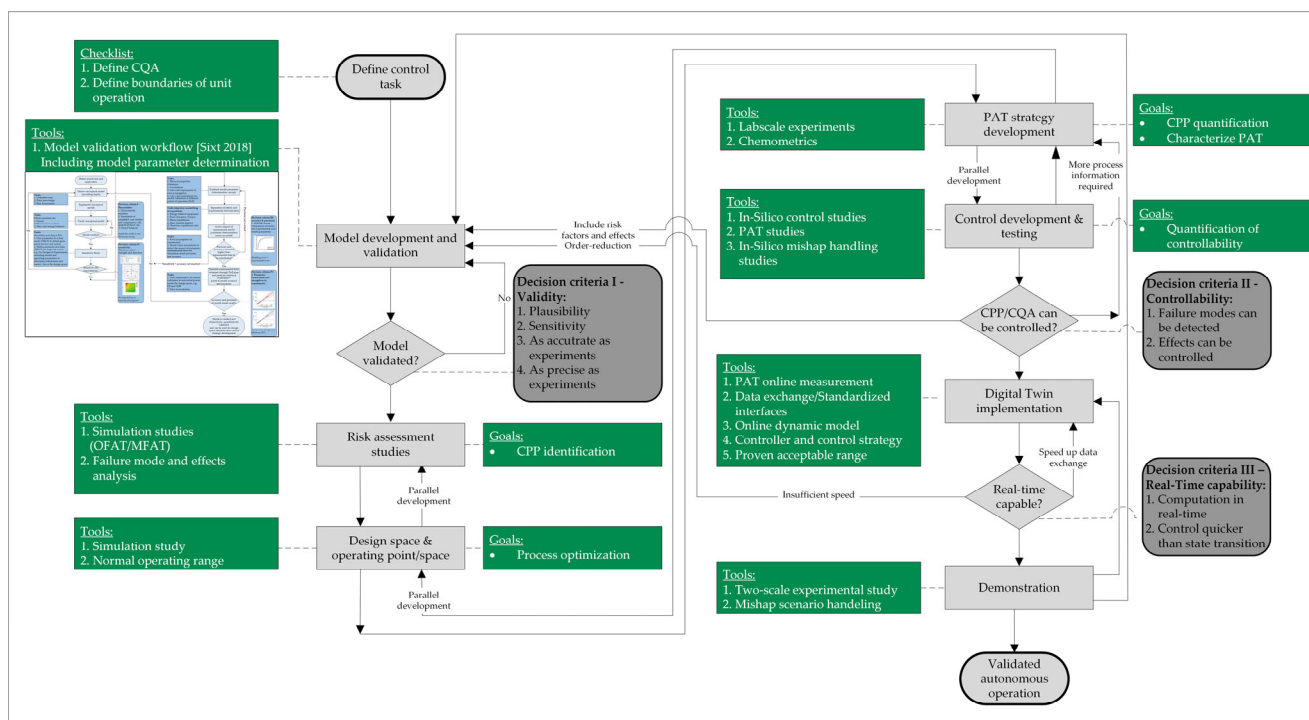


Figure 2. Workflow for the development and validation of digital twins [12,39].

Model predictive control has been established successfully in the chemical and pharmaceutical industries and has proven to outperform conventional PID control [45–47]. Specific applications have been developed and tested in simulations [48,49] and implementation was successful in the laboratory [50] and production environment [51]. Therefore, widespread adaptation of model predictive control in the industry has started and could continue in the future.

2. Material and Methods

2.1. Model Development

2.1.1. Model Equations

The basic path of the substances represented in this model is from absorption on the plant material, to a solute in the aqueous bulk phase, to evaporation, to condensation to an oil phase in the settler. In the bulk phase of the hydrodistillation, a thermodynamic equilibrium is established between the concentration in the laminar boundary layer around the particle and the loading on the particle. This thermodynamic equilibrium of the loading/discharging of the plant particles is represented by a Langmuir isotherm (Equation (3)) [52].

$$q_i(t) = q_{max,i} \cdot a \cdot \frac{K_{L,i} \cdot c_{w,i}(t)}{1 + K_{L,i} \cdot c_{w,i}(t)} \quad (3)$$

Here q_i is the loading of component i , $c_{w,i}$ is the concentration in the laminar boundary layer, K_L is the Langmuir coefficient, $q_{max,i}$ is the maximum loading and a is the capacity factor. This form of the Langmuir isotherm has already been used by Sixt to simulate extraction processes in percolation [39].

The mass transfer to the aqueous bulk phase is modeled with Equation (4). This depends on the particle surface A_p , the mass transfer coefficient $k_{f,i}(T)$ and the concentration gradient between the boundary film $c_{w,i}$ and the solution in the flask $c_{B,i}$.

$$\dot{m}_{i,Extraction} = k_{f,i}(T) \cdot A_p \cdot (c_{B,i}(t) - c_{w,i}(t)) \quad (4)$$

At temperatures below 100 °C, no extraction from the plant material was observed. To mimic this, temperature dependence of the mass transfer coefficient is assumed. This is mapped in Equation (5) using an Arrhenius-based kinetic approach. The kinetic parameters A_i and D are introduced within Equation (5) [53].

$$k_{f,i}(T) = A_i \cdot \exp\left(-\frac{D}{T_{Flask}}\right) \quad (5)$$

The heat balance of the flask is shown in Equation (6). The change of heat in the bubble Q_B is described by the heat fluxes \dot{H} of the water and the components i as well as the evaporation heat of the water \dot{Q}_{Evap} . The heat input $\dot{Q}_{Heating}$ over is described by Equation (6). The heat loss \dot{Q}_{Loss} is assumed to be negligible for simplicity, all inefficiencies are covered by the heat transfer coefficient k furthermore the heat transfer area is assigned the symbol A .

$$\frac{\partial Q_B}{\partial t} = \dot{H}_{H2O,in} - \dot{H}_{H2O,out} + \dot{H}_{i,in} - \dot{H}_{i,out} + \dot{Q}_{Heating} - \dot{Q}_{Evap} - \dot{Q}_{Loss} \quad (6)$$

$$\dot{Q}_{Heating} = A \cdot k \cdot (T_{Heater} - T_{Flask}) \quad (7)$$

From the solution of the heat balance, the evaporation rate of the water $\dot{m}_{H2O,evap}$ can be calculated. This is used in Equation (8) to calculate the evaporation rates of the components. For this, the material data saturated vapor pressure p_0 and the molar mass M_i are required. Furthermore, an evaporation efficiency η is introduced [38].

$$\dot{m}_{oil,Evap} = \dot{m}_{H2O,evap} \cdot \frac{p_{0,i}}{p_{0,tot} - p_{0,i}} \cdot \frac{M_i}{M_{H2O}} \cdot \eta \quad (8)$$

The evaporated components are completely condensed in the condenser. An oil phase forms in the separator, which is in equilibrium with the hydrolyte. This is shown in

Equation (9). The concentrations of components i in the aqueous hydrolate phase $c_{aq,i}$ and the organic oil phase are in equilibrium via the partition coefficient $K_{LLE,i}$ [54].

$$K_{LLE,i} = \frac{c_{org,i}}{c_{aq,i}} \quad (9)$$

Equation (10) shows the mass balance of the separator with the mass flows \dot{m} . Complete phase separation can be assumed in the separator. Thus, in the mass balance of the separator, the mass flow of the target and secondary components from the separator $\dot{m}_{i,out}$ is negligible. To model inefficiencies of the separator, the coefficient ε is introduced here in Equation (11). This coefficient represents the settling efficiency.

$$\frac{\partial m_S}{\partial t} = \dot{m}_{H_2O,in} - \dot{m}_{H_2O,out} + \dot{m}_{i,in} - \dot{m}_{i,out} \quad (10)$$

$$\dot{m}_{i,out} = (1 - \varepsilon) \cdot \dot{m}_{i,in} \quad (11)$$

2.1.2. Model Parameter Determination

The model parameters are divided into kinetic and equilibrium parameters. These are determined experimentally. The equilibrium parameters of the isotherms are performed via extraction with PHWE. This is performed exhaustively for the determination of maximum loading. For the equilibrium parameter K_L is performed with different volumes of solvent to quantify the shift in equilibrium between the concentration in the solvent and the loading of the plant material. Tempered shaking experiments are performed to determine the liquid–liquid equilibrium parameter. A summary of the methodology is shown in Figure 3.

Model Parameter Determination

1. Fluid Dynamics

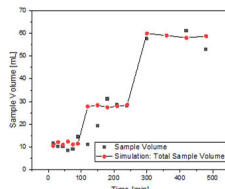
1.1 Ideal Stirring Vessel

$$F(t) = \frac{c(t)}{c_0} = 1 - \alpha \cdot \exp\left(-\frac{\alpha}{\beta} \cdot \frac{t}{\tau}\right)$$

$$\text{Dead volume:} \quad 1 - \beta$$

$$\text{Short-circuit flows:} \quad 1 - \alpha$$

2. Energy Balance

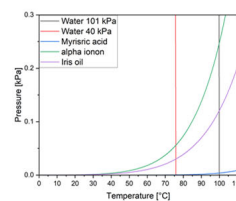
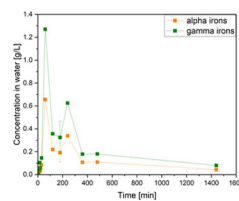


$$\dot{Q}_{\text{Heating}} = A \cdot k \cdot (T_{\text{Heater}} - T_{\text{Flask}})$$

3. Phase Equilibrium:

3.1 LLE - Shake Flask

3.2 VLE – Hausbrand Diagram



$$m_{cond,i} = c_{org,i} \cdot V_{org} + c_{aq,i} \cdot V_{aq}$$

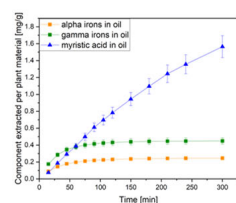
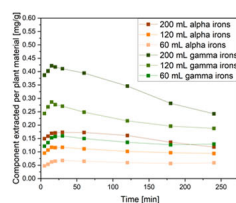
$$K_{LLE,i} = \frac{c_{org,i}}{c_{aq,i}}$$

$$i(c_{p,i}(r, t)) = q_{max,i} \cdot a \cdot \frac{K_{L,i} \cdot c_{p,i}(r, t)}{1 + K_{L,i} \cdot c_{p,i}(r, t)}$$

4. Kinetics

4.1 PHWE Lab scale

4.2 Hydrodistillation Lab Scale



$$k_f(T) = A \cdot \exp\left(-\frac{D}{T_{\text{Flask}}}\right)$$

$$\dot{m}_{i,Extraction} = k_f \cdot A_p \cdot (c_{i,Flask}(t) - c_{i,w}(t))$$

$$\dot{m}_{oil,Evap} = \dot{m}_{H_2O,out} \cdot \frac{p_{0,org}}{p_{0,tot} - p_{0,org}} \cdot \frac{M_{org}}{M_{H_2O}} \cdot \eta$$

Figure 3. Summary of the model parameter determination concept.

The kinetic parameters are determined by hydrodistillation. The parameter η introduced in the Hausbrandt-based evaporation rate of oil components is set to the value 1. The mass transfer parameter k_f is calculated from the temperature-dependent Arrhenius

approach. For the determination of the Arrhenius parameters, hydrodistillations are carried out at different heating behaviors. For this purpose, the sheath temperature is varied. The model can then be used to estimate these parameters. Heat transfer coefficients are obtained from the documented literature data [55].

GC Analysis

An internal alpha ionone standard (Sigma–Aldrich, St. Louis, MO, USA) is first added to the aqueous samples generated in the model parameter determination experiments so that a concentration of 0.05 g/L internal standard is present in the respective sample. Then, using liquid–liquid extraction with hexane at a ratio of 1:1 *v/v*, both the irons and the fatty acids are extracted from the aqueous phase into the organic phase. The organic phase is then analyzed in a gas chromatograph using a VF-5ms column from Agilent Technologies, Inc. (Santa Clara, CA, USA) and helium as carrier gas at 300 °C with an FID-Detector, according to Hoess [29].

Isotherm Determination

The parameters of the adsorption isotherms are determined by pressurized hot water extraction (PHWE) [56,57]. For this purpose, one PHWE is run on a laboratory scale (10 × 100 mm column, 1 g plant material) in a circulating mode at 120 °C and 1 mL/min and five different volumes. The equilibrium concentration is determined after 4 h in each case. The total content is determined by running an exhaustive laboratory-scale PHWE (10 × 100 mm, 1 g plant material) at also 120 °C and 1 mL/min for 24 h and sampling after 10, 20, 30, 45, 30, 60, 120, 150, 180, 240, 360, 480, and 1440 min, respectively. The samples are then analyzed by GC analysis for their iron and fatty acid content.

Liquid–Liquid Equilibrium

The partition coefficient of the oil phase is determined by equilibrating previously analyzed iris butter samples and a purchased alpha iron standard (Sigma-Aldrich) with water at 99 °C in a thermal shaker. The concentration of this, and the concentration of fatty acids in the aqueous phase are determined by GC analysis after equilibration.

Hausbrand Diagrams

Hausbrand Diagrams were calculated according to Baerns et al. [58] using NRTL for nonpolar components and UNIQUAC for polar components.

3. Results

3.1. Model Precision

To determine the accuracy of the model and the described model parameter determination concept, a Monte Carlo simulation study was performed. The model parameters were randomly varied by the determined model parameters. The relative limits of the model parameters are shown in Table 1. For this simulation study, 250 simulations were conducted.

Table 1. Ranges of the model parameter varied in the Monte Carlo simulation study.

Model Parameter	Deviation
Heat Transfer Coefficient	±25%
Arrhenius Parameter	±5%
Henry Coefficient	±15%
Maximum Loading	−2.5%; +15%
LLE Distribution Coefficient	±10%
Nitsch Coefficient	±25%

For the evaluation of this study, the relative deviations of the extraction curves of the major and minor components in the oil and the hydrolate were investigated. At the end

of the extraction, a standard deviation of these values was calculated from all simulations. These were compared with the standard deviations from the experiments at the laboratory plant, and are listed in Table 2. The relative standard deviations of the investigated process attributes in the simulation study are comparable to the deviations in the experimental test series. Thus, the model can represent these as shown in the experiments and can be considered precise.

Table 2. Results of the Monte Carlo simulation study in comparison with the deviation in the experimental studies.

Model Result	Deviation in Simulation	Deviation in Experiments
Concentration of Irones in Hydrolate	±11.2%	±12%
Concentration of Myristic Acid in Hydrolate	±5%	±7.5%
Extracted Irones in Oil	±17.5%	±13%
Extracted Myristic Acid in Oil	±15%	±18%

3.2. Model Accuracy

Several experiments were performed to determine the accuracy of the model. The hydrodistillation was performed with different configurations and scales. By this procedure also a proof of the scale transfer can be shown. In addition, the different configurations can be used to evaluate individual elements of the model.

The first configuration is open hydrodistillation. In this, the hydrolate from the separator is not returned to the flask. Instead, the sample is collected and analyzed in a separate container. After the pre-determined sampling time has been reached, new water is added to the flask to prevent the plant material from drying out or burning. The process is interrupted for a short time.

As shown in Figure 4, the extraction curves of the main components can be well represented by the model. The most important curve here is Figure 4a, since the yield of the main components from the extracted oil is shown here relative to the mass of the plant material. This is very well matched with the determined model parameters ($R^2 = 0.995$). The concentration of the components in the hydrolate shows a high experimental inaccuracy due to the low concentrations and, therefore, there are high error margins on the detecting element of the offline analytics. The major and minor components are isolated from the collected hydrolate by liquid–liquid extraction and quantitatively determined by gas chromatography. This is shown in Figure 4b. For the myristic acid, the data can be found in Figure 4c. Here, the cumulative yield from the oil is well matched ($R^2 = 0.986$), but the concentration later in the extraction is underestimated ($R^2 = 0.882$). One explanation for this may be that small parts of the oil were sponged into the sample vessel of the hydrolate. This may be due to the larger sample volumes towards the end of the extraction process. The components are extracted with an organic phase from the hydrolate, this can also dissolve entrained droplets. This may also explain the slight underestimation of the alpha-irone from the hydrolate. This inaccuracy is smaller than that of the myristic acid, because the myristic acid is extracted later than the alpha-irone, so in the larger hydrolate samples the extraction of the irone is almost complete. Figure 4d includes the sample volume in the experiments and simulation; this information shows accuracy in the heating and evaporation of the hydrodistillation.

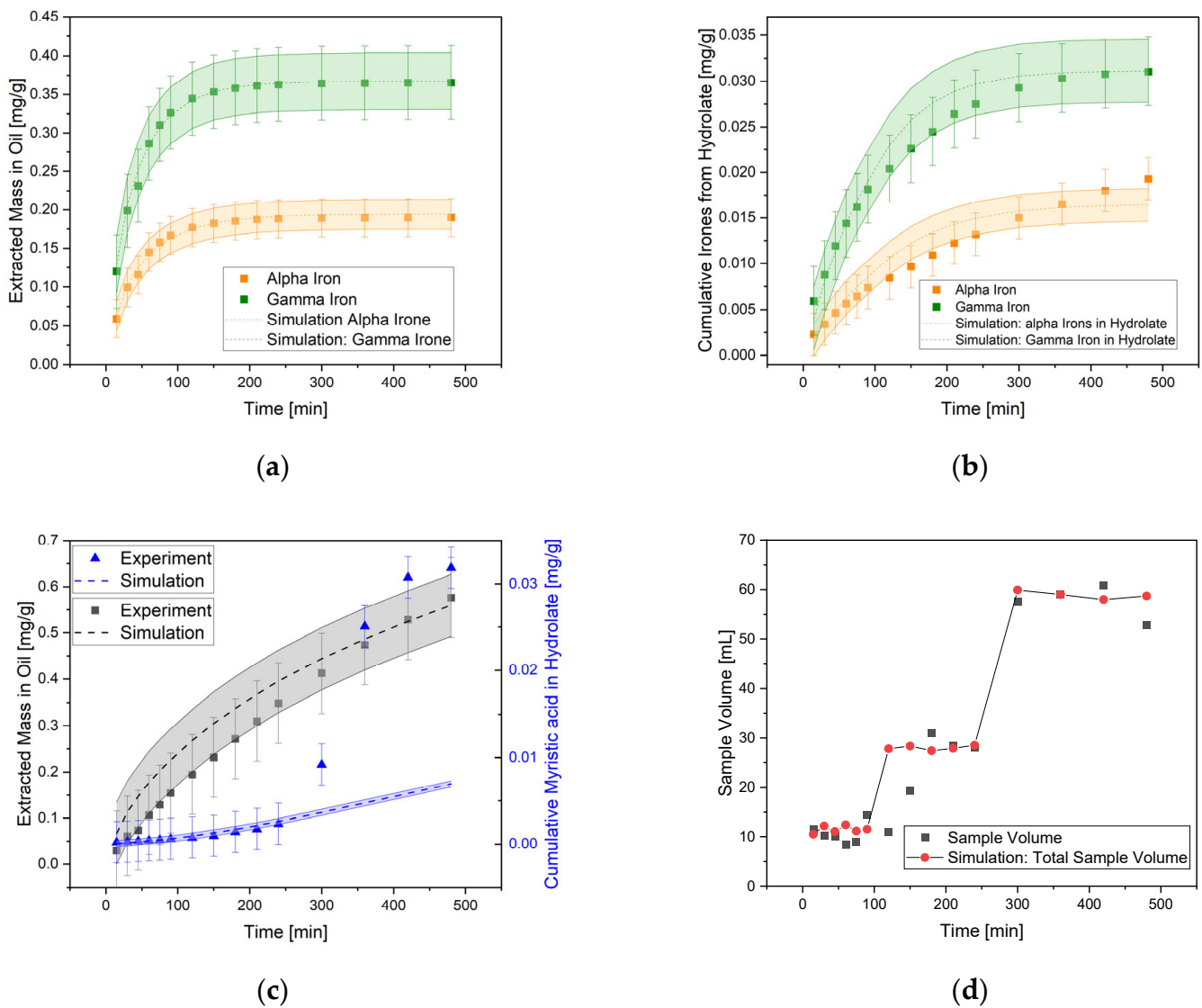
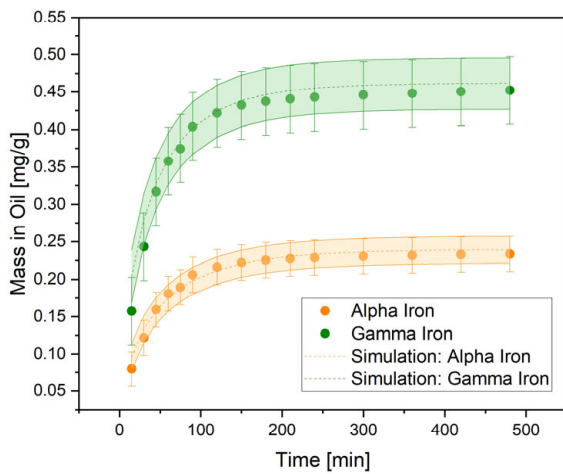
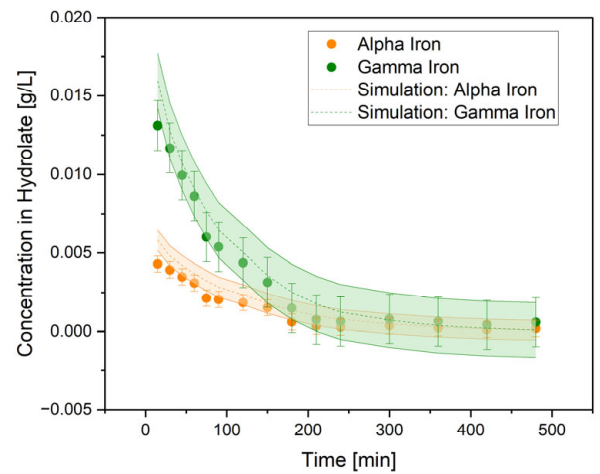


Figure 4. Time-dependent simulated and experimental results of the extracted irone mass (a), cumulative irones from hydrolate (b), myristic acid in hydrolate and oil (c) and volume of the sample (d).

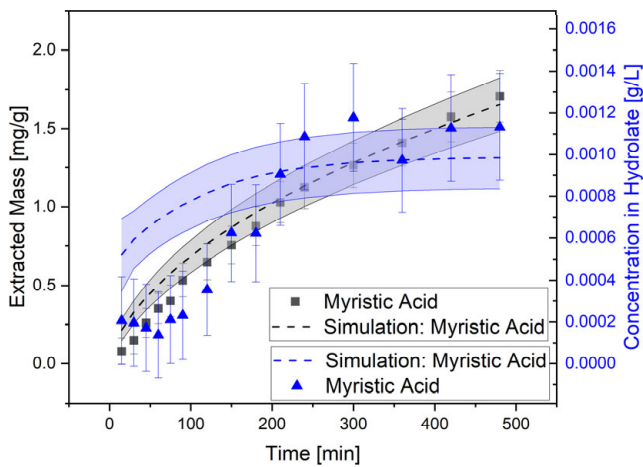
The results of the second configuration, the closed process, is shown in Figure 5. Here, the hydrolate from the separator is returned directly to the flask. Sampling takes place while the process is briefly interrupted. In this process, the hydrolate and oil are removed separately from the separator. As a result, the sample volumes of the hydrolate are much smaller than in the open experiments. Here, as shown in Figure 5b, the experimental values are better reproduced by the model ($R^2 = 0.964$). The extraction process of the myristic acid shown in Figure 5c is also well matched ($R^2 = 0.969$).



(a)



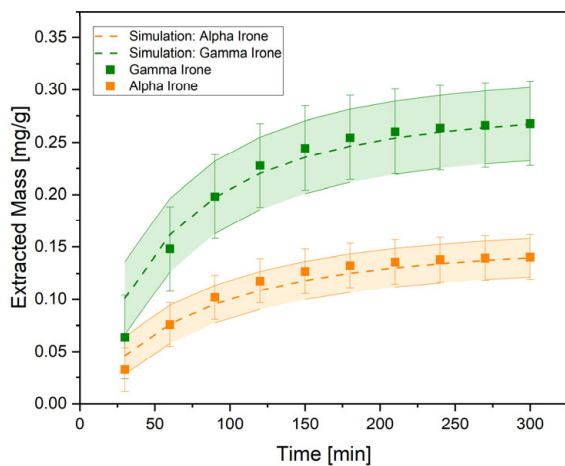
(b)



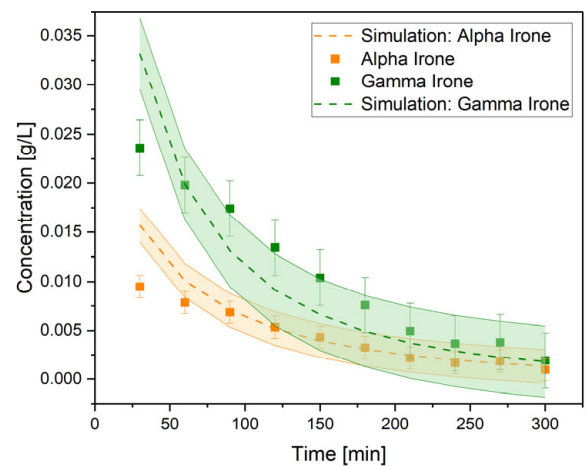
(c)

Figure 5. Time-dependent simulated and experimental results with a closed loop configuration on the small lab scale of the extracted iron mass (a), cumulative irones from hydrolate (b), myristic acid in hydrolate and oil (c).

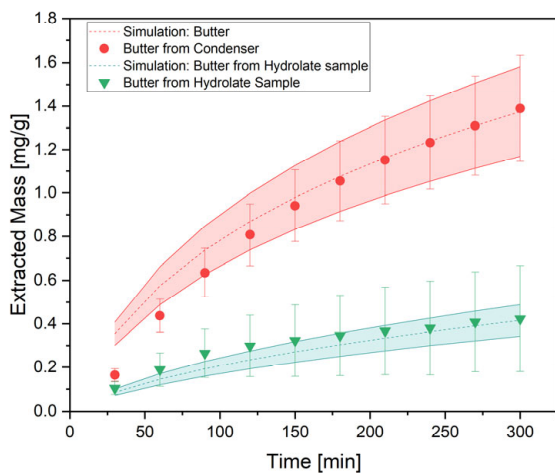
In the closed configuration, hydrodistillation was carried out on the next higher scale. The mass of plant material and the volume of water used were increased tenfold. The extraction curves are shown in Figure 6. Due to the analytical method used here for the target component determination, a very large volume of hydrolates was extracted. As in the open configuration, this resulted in some droplets of oil being entrained in the sample and this affected the quality of the model. Nevertheless, a coefficient of determination for the concentration in the hydrolate of the target components of $R^2 = 0.844$ was found. The simulated progression of the components into the oil phase agrees well with that measured in the experiments. In addition, myristic acid was well represented by the model.



(a)



(b)



(c)

Figure 6. Time-dependent simulated and experimental results with a closed loop configuration on the large lab scale of the extracted iron mass (a), cumulative irones from hydrolate (b), butter in hydrolate and oil (c).

Furthermore, the pilot plant was simulated. This is operated with 5 kg of the plant material and thus represents a scale extension of $200\times$. In this specific plant, incomplete separation of the organic and aqueous phases occur in the separator during operation. This leads to losses of the yield. This is readjusted with the efficiency factor ε . Since the process flow of this plant was also well simulated by the model, this parameter can also be determined well and a scale transfer can be ensured. The simulated and experimental processes are shown in Figure 7.

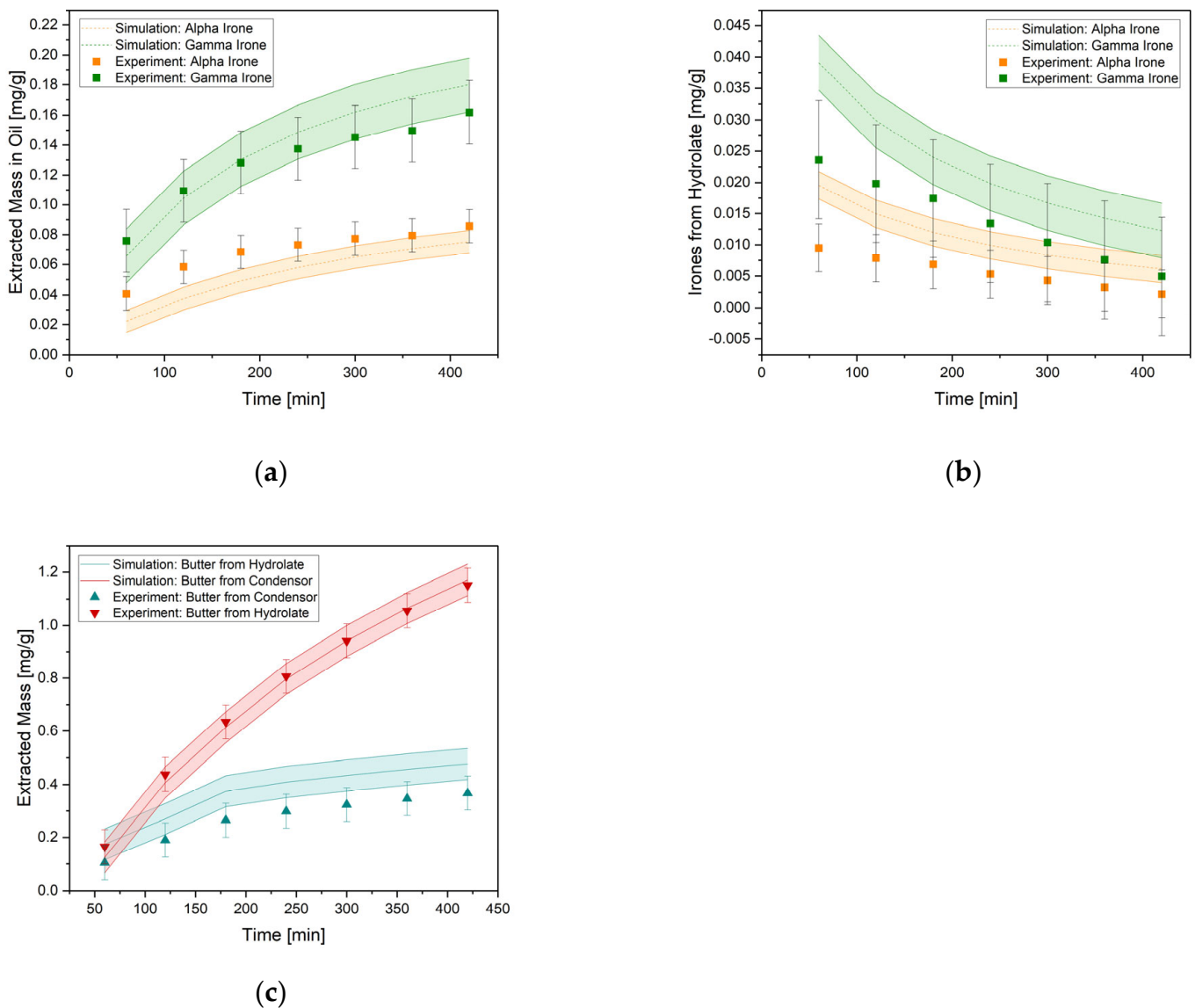


Figure 7. Time-dependent simulated and experimental results with a closed loop configuration on the pilot plant scale of the extracted iron mass (a), cumulative irones from hydrolate (b), butter in hydrolate and oil (c).

3.3. Risk Assessment and PAT Development

3.3.1. Risk Assessment and Failure Mode and Effect Analysis (FMEA)

For the operator of the process, the most important quality attributes are the yield of the main component and the purity. For the economic efficiency of the process, the productivity and the energy consumption are determined as process attributes. In the context of QbD-based process development, the process and the control of this process should be designed in a way in which these critical quality and process attributes can be well controlled. For this purpose, a one-factor-at-a-time (OFAT) simulation study was first conducted. The operating parameters are varied individually in order to determine the most sensitive ones. These are ranked according to the strength of the parameter's influence on the CQA or PA. This is shown in Figure 8. Furthermore, a multiple-factor-at-a-time (MFAT) simulation study is performed. Here, the operating parameters are varied within the same limits according to a static experimental design in order to quantify the interactions of the operating parameters with each other and their influence on the CQA and PA.

	Impact CQA (Yield)	Impact CQA (Purity)	Impact PA (Productivity)	Impact PA (Energy used)	Highest main effect score	Interaction CQA (Yield)	Interaction CQA (Purity)	Interaction PA (Productivity)	Interaction PA (Energy used)	Highest interaction effect score	Severity
Target Component Content	8	8	8	1	8	4	2	4	1	4	32
Side Component Content	4	8	1	1	8	2	1	1	1	2	16
Material mass	8	4	8	1	8	2	2	4	1	4	32
Solvent : Plant Ratio	1	1	1	1	1	1	2	1	1	2	2
Settler inefficiency	8	8	8	1	8	1	2	4	1	4	32
Coolent temperature	4	1	1	4	4	2	2	1	1	2	8
Coolent Flow rate	1	1	1	4	4	1	1	1	1	1	4
Heat transfere area	1	1	1	4	4	1	1	1	1	1	4
Heat transfere efficiency	1	1	1	8	8	1	1	1	1	1	8

Figure 8. Results of the risk assessment study and identification of the sensitive process parameters (from most sensitive in red to least sensitive in green).

A total score is calculated from the combination of the sensitivities from OFAT and MFAT. For the hydrodistillation result, the most sensitive parameters are the content of the target components in the plant material, the mass of plant material used and the efficiency in the separator. This result is in good agreement with results obtained from the experimental studies. When the content of target components in plant material is high, high yield and productivity can be achieved and when more plant material is used, the productivity of the process can increase. In addition, the efficiency of the separator can strongly affect the yield of the process if parts of the product flow back into the flask. The sensitive process parameters determined here must be made detectable in the next step of the PAT strategy and regulated with a control strategy so that the CQA and PA remain within the specified limits.

3.3.2. PAT Strategy Development

The quantitative determination of the target components and the minor components of the samples is carried out by means of an established gas chromatography method. Different chromatograms of the samples of the oil phase during extraction are shown in Figure 9. The goal of establishing the PAT measurement technique in the course of Quality by Design-based process development is the online monitoring of the concentration of the components. Spectroscopic measurement methods such as FTIR (Mettler Toledo, ReactIR 702 L, Micro Flow Cell, Columbus, OH, USA) and DAD (Knauer, Smartline UV Detector 2600, Berlin, Germany) are suitable for this purpose.

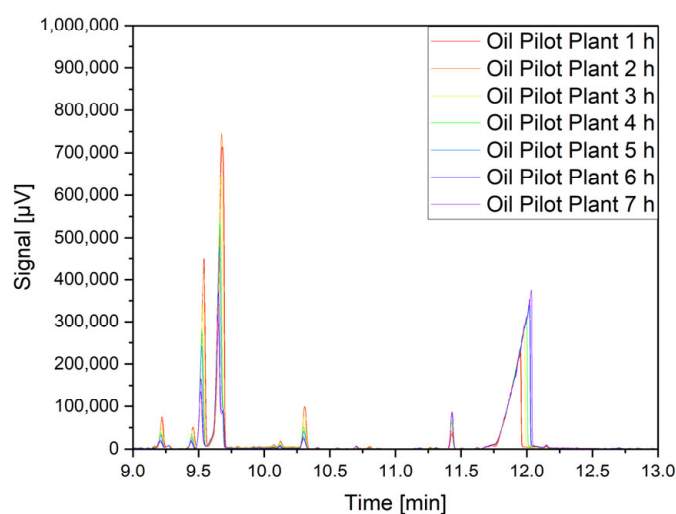


Figure 9. GC-Chromatograms of oil samples during extraction in pilot plant.

In the context of this work, DAD is used to monitor the concentration of the irons in the hydrolate, since these are only present in very low concentrations in the hydrolate. Here, the progress of the extraction can be observed, but the purity of the product cannot

be determined by the concentration of the fatty acids. Accuracies of $R^2 = 0.922$ for alpha irons and $R^2 = 0.976$ for gamma irons in hydrolate can be achieved via PLS-Regression (Figure 10). For online monitoring of the irons in hydrolate, a multiple scatter correction of the DAD spectrum from 190–330 nm was used.

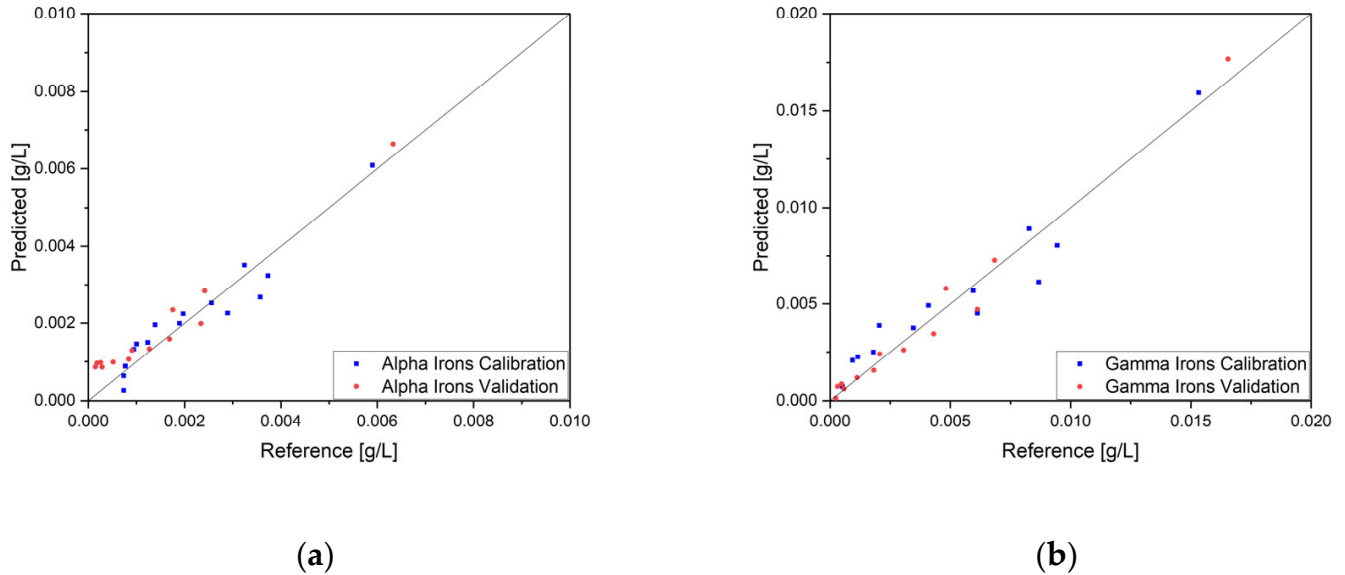


Figure 10. Predicted vs. reference plot of alpha (a) and gamma (b) irons in hydrolate calculated via PLS-regression using DAD spectra.

FTIR is used to monitor the composition of the essential oil. Here, a high concentration of irons is desired, whereas the concentration of fatty acids should be kept low. As the extraction proceeds, the concentration of irons decreases. The dominant fatty acid, myristic acid, on the other hand, increases as the extraction progresses, resulting in a deterioration of the purity of the target product (Figure 11). Here, the target components can be determined online with an accuracy of $R^2 = 0.988$ for alpha irons and $R^2 = 0.996$ for gamma irons and the minor component myristic acid with an accuracy of $R^2 = 0.972$ of the PLS-Regressions (Figure 12). To determine the concentration of irons in oil the FTIR spectrum from $1750\text{--}1580\text{ cm}^{-1}$ was used. For the determination of myristic acid in oil the oil phase the part from $3000\text{--}2800\text{ cm}^{-1}$ was used after first order derivation.

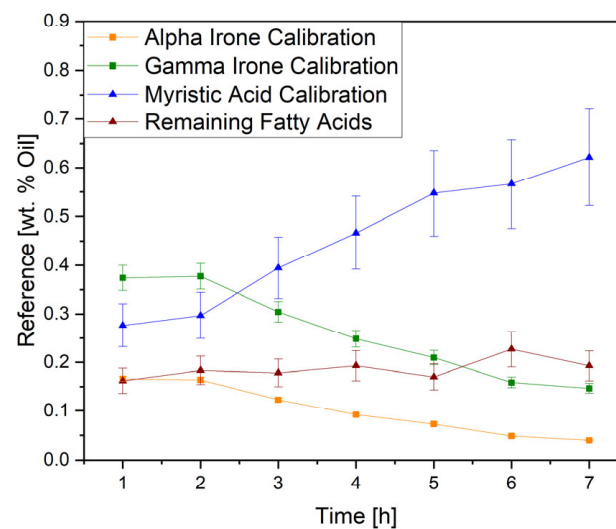


Figure 11. Time course of oil composition during extraction in pilot plant.

of the ingredients is not known, the extraction time is fixed when the process is designed and is no longer adjusted. Thus, any irregularities in the plant material directly affect the performance of the process.

The goal of the digital twin is to compensate for these fluctuations. For this purpose, the digital twin must have the information of the content. This is determined by estimation from the PAT signals using a proprietary algorithm, which is based on the model from Section 2.1. To determine the accuracy of this estimation routine, it is tested with a simulation study. For this purpose, the extraction courses and their PAT signals were simulated with the inaccuracies from the PAT development. From the simulated PAT signals, the digital twin is now to estimate the initial loading of the plant material. Here, the PAT signals of the 10%, 25%, 50%, 75%, and 100% of the extraction time were provided to the digital twin.

Figure 14 shows the coefficient of determination and the mean deviation from the true content of the target and minor components. As expected, the regression quality increases with the time course, since more relevant information of the extraction course is available to the digital twin. For both, the concentration course from the DAD signal and the extraction course from the FTIR signal, a low deviation to the true value can be achieved after 25% of the extraction time from all simulations. For the system of FTIR and level measurement a deviation of 7.2% can be calculated. Since this is the more comprehensive system with which the purity of the product can also be determined online, it is used for the control studies. If the digital twin is only to be used for the determination of the irone extraction, the FTIR can be dispensed with and a similar accuracy can only be achieved with the DAD.

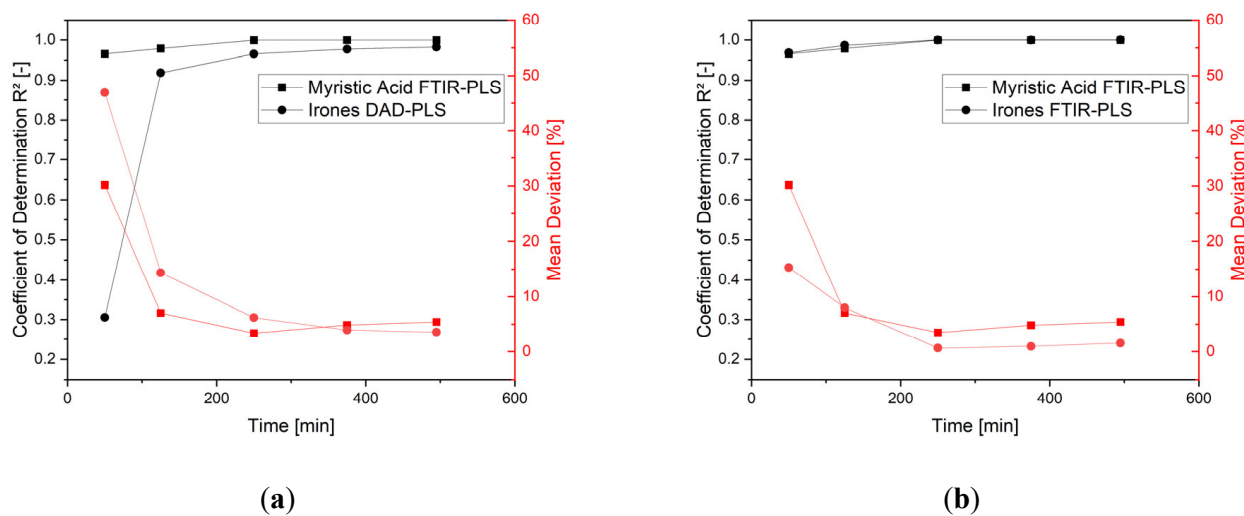


Figure 14. Coefficient of determination (in black) and mean deviation (in red) of estimation of plant material content by the digital twin for the PAT-System of DAD and FTIR (a) and FTIR alone (b).

3.5. Control Strategy Assessment

For the control study and the comparison of the control systems and driving modes, a traditional driving mode is first used as a reference. The purity and productivity is shown in Figure 15 depending on the extraction yield. This is a simulated run, where the plant material has three times the minimum irone content. This is the case where the longest extraction time is required. Hereby, an operating point is selected, at which the highest possible purity and productivity is achieved at a high yield. If the extraction is run longer, the purity and productivity will decrease non-linearly. The operating point for this extraction is an extraction time of 290 min.

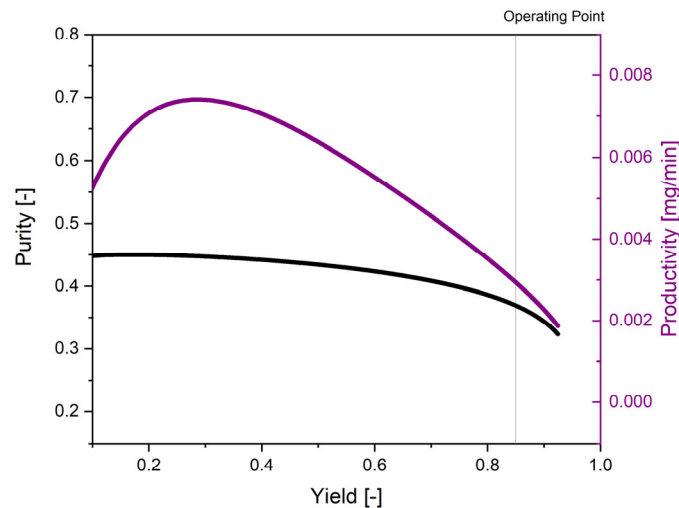


Figure 15. Dependence of the product purity (in black) and the process productivity (in purple) on the yield of the target components.

For the control studies, different disturbances of the process were simulated. The amount of plant used, the content of the plant material, the efficiency of heat transfer at the flask and condenser, the efficiency of the separator, and the volume of water in the FMEA interfaces were varied. These components were simulated using the traditional operating mode and the digital twin. For the digital twin, three different settings were tested, one was set to not go below a purity of 0.37 mg/mg and the other was set to high productivity. The last variant was chosen to maximize the yield. The results of this simulation study are shown in Figure 16.

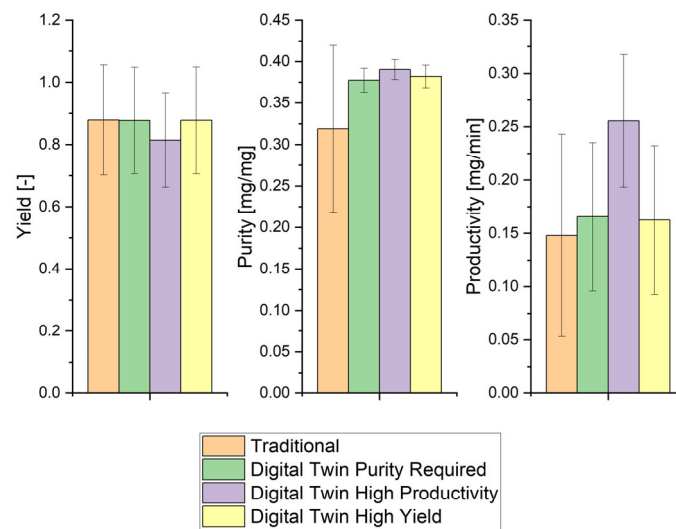


Figure 16. Comparison of the process control systems and their influence on the key process figures.

For a given purity of the product, the DT specification can be met very well. It is also noticeable that the variance of the purity values is much lower than in the traditional mode. This reduction by a factor of eight can be attributed to the presence of process information, which is also the objective of the mode of operation according to the specified purity. In the high-productivity mode, a 40% increase in hydrodistillation productivity was simulated. This could also be achieved with the variant for which a high yield was assumed, and yet a process productivity increase of 9.4% was achieved without a significant loss in yield. Since current process information is used, the digital twin can terminate the process when extraction is complete.

4. Discussion

It could be shown that, with the digital twin, higher productivity can be achieved while maintaining the same yield. The same system can also be used to specify purity requirements for the product. Online monitoring with the PAT system and the model-based prediction mean that these requirements can be met very precisely. Thus, an upgrading of the product already takes place during the extraction and production costs can be saved in the downstream processing.

Hydrodistillation is a very energy-intensive extraction process, since a large volume of water must be continuously evaporated and condensed. Therefore, the maxim is true: unnecessary process time must be avoided. The process time is directly reflected in the GWP emitted in the process. Furthermore, an increase in extraction productivity can directly lead to a reduction in CoGs. In the comparison of the control strategies and operation modes, these values are shown relative to those of the traditional operation mode in Figure 17. With the digital twin, a reduction in GWP of up to 46.5% and a reduction in CoGs of up to 22.4% could be achieved. Even with a similarly good yield to the traditional driving method, a reduction of GWP by 9.4% and CoGs by 19.7% can be expected.

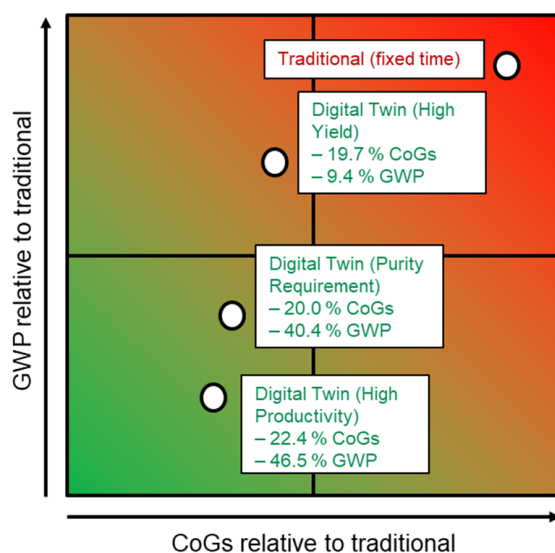


Figure 17. Comparison of the process control strategies based on GWP and CoGs.

Through the study, the process could be better understood, thus a step towards higher efficiency and energy savings has already been taken. Another step is the implementation of PAT for monitoring and decision making during the process. This can already bring a significant advantage in the extraction process. To enable the autonomous operation of the process, the digital twin is implemented, so that the process can reliably achieve very good results.

5. Conclusions

This work has shown that the potential of model predictive control via digital twin for hydrodistillation can achieve a reduction in ecological footprint by up to 46.5%, while also reducing the cost of production by 22.4%. As shown in Section 1.3, model predictive control has been developed and implemented in an industrial environment. These findings are in line with previous studies [12,50].

Digital twin technology can reduce operator workload, due to its ability to monitor and control the hydrodistillation process in real time. This can further increase the economic viability of this green extraction process. Automation in chemical and pharmaceutical processes is strived for because of its economic advantages [60–62].

The approach shown is ready for industrialization and reduces the cost of goods and global warming potential equivalent towards worldwide competitiveness and political demand for climate neutrality significantly as no other technology exists. Nevertheless, decision makers seem to see drawbacks in unclear business cases and lack comprehension. Both obstacles could be overcome by:

- A business case for additional investments of about €100,000 to less than 1 mio. € with annual additional maintenance cost of less than €100,000 are easily financed by factor 2–5 CoGs reduction with payout time of about 1 year.
- Increasing the number of available skilled employees or training courses available to overcome the potential lack of comprehension.

Author Contributions: Conceptualization, J.S.; methodology, A.U. and A.S.; software, A.U.; validation, A.S., L.K., T.H. and M.F.; formal analysis A.U., L.K., T.H. and M.F.; investigation, L.K., T.H. and M.F.; resources, T.H. and M.F.; writing—original draft preparation, A.U., L.K. and A.S.; writing—review and editing, M.F. and J.S.; visualization, A.U. and L.K.; supervision, J.S.; project administration, J.S.; funding acquisition, J.S. All authors have read and agreed to the published version of the manuscript.

Funding: The authors want to gratefully acknowledge the Bundesministerium für Wirtschaft und Klimaschutz (BMWK), especially Michael Gahr (Projekträger FZ Jülich), for funding their scientific work.

Data Availability Statement: Data are contained within the article.

Acknowledgments: The paper is dedicated to Farid Chemat, whom J.S. did have the honor to get known first at GENP conference 2013 in Avignon, which Farid organized. His warm welcome and enthusiasm towards green extraction has been infectious since. The community has lost a sound researcher, a pushing driver of common actions and we a good friend. Our thoughts are with his family. The authors would like to thank the whole team of the institute for their valuable contributions and their partners in many industrial applications. Especially Frank Steinhäuser, Colin Herzberger and Janek Wienert for their support in the laboratory. For his assistance and knowledge during this and other projects the authors thank Martin Tegtmeier. And for his help with analytical technologies the authors thank Jan C. Namyslo of TU Clausthal Organic Chemistry Department.

Conflicts of Interest: Authors Theresa Höß and Marcel Flemming are employed by the company SKH GmbH. The remaining authors declare that the research was conducted in the absence of any commercial or financial relationships that could be construed as a potential conflict of interest.

Abbreviations

AD	Anno domini
APC	Advanced process control
API	Active pharmaceutical ingredient
CoGs	Cost of goods
CPP	Critical process parameter
CQA	Critical quality attribute
DAD	Diode array detector
DT	Digital twin
FID	Flame ionization detector
FMEA	Failure mode and effect analysis
FTIR	Fourier-transformed infrared spectroscopy
GC	Gas chromatography
GWP	Global warming potential
l/l	Liquid to liquid ratio
LLE	Liquid-Liquid-extraction
MFAT	Multiple-factor-at-a-time
NRTL	Non-Random-Two-Liquid-Model
OFAT	One-factor-at-a-time

PAT	Process analytical technology
Ph. Eur.	European Pharmacopoeia
PHWE	Pressurized hot water extraction
PLS	Partial least squares regression
QbD	Quality by Design
s/l	Solid to liquid ratio
SLE	Solid-Liquid-Extraction
UNIQUAC	Universal Quasichemical

Symbols

A	Heat transfer area
A_i	Arrhenius parameter
A_p	Area of particle
a	Capacity factor
$c_{B,i}$	Concentration in bulk phase
$c_{w,i}$	Concentration in boundary layer
D	Arrhenius exponent
\dot{H}	Enthalpy flux
$k_{f,i}$	Mass transfer coefficient
$K_{L,i}$	Langmuir coefficient
$K_{LLE,i}$	partition coefficient
\dot{m}	Mass flux
M	Molar mass
$p_{0,i}$	Saturation vapor pressure
Q	Heat
q_i	Loading
$q_{max,i}$	Maximum loading
T	Temperature
ε	settling efficiency
η	evaporation efficiency

References

1. Chemat, F.; Abert-Vian, M.; Fabiano-Tixier, A.S.; Strube, J.; Uhlenbrock, L.; Gunjevic, V.; Cravotto, G. Green extraction of natural products. Origins, current status, and future challenges. *TrAC Trends Anal. Chem.* **2019**, *118*, 248–263. [[CrossRef](#)]
2. Jeliakov, V.D.; Cantrell, C.L. (Eds.) *Medicinal and Aromatic Crops: Production, Phytochemistry, and Utilization*; American Chemical Society: Washington, DC, USA, 2016; ISBN 9780841231276.
3. Burger, P.; Plainfossé, H.; Brochet, X.; Chemat, F.; Fernandez, X. Extraction of Natural Fragrance Ingredients: History Overview and Future Trends. *Chem. Biodivers.* **2019**, *16*, e1900424. [[CrossRef](#)]
4. Herrera-Rodríguez, S.E.; Pacheco, N.; Ayora-Talavera, T.; Pech-Cohuo, S.; Cuevas-Bernardino, J.C. *Advances in the Green Extraction Methods and Pharmaceutical Applications of Bioactive Pectins from Unconventional Sources: A Review*; Elsevier: Amsterdam, The Netherlands, 2022; pp. 221–264. ISBN 9780323910972.
5. Tufvesson, L.M.; Tufvesson, P.; Woodley, J.M.; Börjesson, P. Life cycle assessment in green chemistry: Overview of key parameters and methodological concerns. *Int. J. Life Cycle Assess.* **2013**, *18*, 431–444. [[CrossRef](#)]
6. Chemat, F.; Strube, J. (Eds.) *Green Extraction of Natural Products*; Wiley: Hoboken, NJ, USA, 2015; ISBN 9783527336531.
7. Herwig, C.; Pörtner, R.; Möller, J. *Digital Twins*; Springer International Publishing: Cham, Switzerland, 2021; ISBN 9783030716592.
8. Gharaie, M.; Zhang, N.; Jobson, M.; Smith, R.; Panjeshahi, M.H. Simultaneous optimization of CO₂ emissions reduction strategies for effective carbon control in the process industries. *Chem. Eng. Res. Des.* **2013**, *91*, 1483–1498. [[CrossRef](#)]
9. Simkoff, J.M.; Lejarza, F.; Kelley, M.T.; Tsay, C.; Baldea, M. Process Control and Energy Efficiency. *Annu. Rev. Chem. Biomol. Eng.* **2020**, *11*, 423–445. [[CrossRef](#)] [[PubMed](#)]
10. He, B.; Bai, K.-J. Digital twin-based sustainable intelligent manufacturing: A review. *Adv. Manuf.* **2021**, *9*, 1–21. [[CrossRef](#)]
11. Bergs, T.; Brecher, C.; Schmitt, R.; Schuh, G. *Internet of Production—Turning Data into Sustainability*; Apprimus Verlag: Aachen, Germany, 2021.
12. Uhl, A.; Knierim, L.; Tegtmeier, M.; Schmidt, A.; Strube, J. Is Regulatory Approval without Autonomous Operation for Natural Extract Manufacturing under Economic Competitiveness and Climate-Neutrality Demands Still Permissible? *Processes* **2023**, *11*, 1790. [[CrossRef](#)]
13. Kockmann, N. 200 Jahre Entwicklung in der kontinuierlichen Destillation. *Chem. Ing. Tech.* **2013**, *85*, 1815–1823. [[CrossRef](#)]

14. Deibele, L. Die Entwicklung der Destillationstechnik von ihren Anfängen bis zum Jahre 1800. *Chem. Ing. Tech.* **1991**, *63*, 458–470. [[CrossRef](#)]
15. Brunschwig, H. *Buch der Wahren Kunst Zu Destillieren*; Sentralantiquariat der DDR: Leipzig, Germany, 1972.
16. Bittel, A. Zur Geschichte multiplikativer Trennverfahren. *Chem. Ing. Tech.* **1959**, *31*, 365–378. [[CrossRef](#)]
17. Blass, E.; Liebl, T.; Häberl, M. Extraktion—Ein historischer Rückblick. *Chem. Ing. Tech.* **1997**, *69*, 431–437. [[CrossRef](#)]
18. Schelenz, H. *Zur Geschichte der Pharmazeutisch-Chemischen Destilliergeräte*; Springer: Berlin/Heidelberg, Germany, 1911; ISBN 978-3-642-98267-5.
19. Gavahian, M.; Farahnaky, A. Ohmic-assisted hydrodistillation technology: A review. *Trends Food Sci. Technol.* **2018**, *72*, 153–161. [[CrossRef](#)]
20. Sela, F.; Karapandzova, M.; Stefkov, G.; Kulevanova, S. Chemical composition of berry essential oils from *Juniperus communis* L. (Cupressaceae) growing wild in Republic of Macedonia and assessment of the chemical composition in accordance to European Pharmacopoeia. *Maced. Pharm. Bull.* **2011**, *57*, 43–51. [[CrossRef](#)]
21. ECA Academy. New Ph. Eur. Chapter on Essential Oils. ECA Academy. 5 June 2020. Available online: <https://www.gmp-compliance.org/gmp-news/new-ph-eur-chapter-on-essential-oils> (accessed on 11 October 2023).
22. Kabuba, J.; Huberts, R. Steam extraction of essential oils: Investigation of process parameters. *Can. J. Chem. Eng.* **2009**, *87*, 915–920. [[CrossRef](#)]
23. Keung Mak, W.C. Comparisons between the Hydro Distillation and the Steam Distillation in the Extraction of Volatile Compounds from and the Anti-oxidative Activity of *Prunella Vulgaris*. *J. Drug Deliv. Ther.* **2022**, *13*, 5955.
24. Wollinger, A. *Application of a Supercritical Carbon Dioxide Extraction Unit—Extraction of *Iris germanica* L. and *Rosmarinus officinalis* L.*; Universität Regensburg: Regensburg, Germany, 2017.
25. Aćimović, M.; Tešević, V.; Smiljanić, K.; Cvetković, M.; Stanković, J.; Kiprovski, B.; Sikora, V. Hydrolates: By-products of essential oil distillation: Chemical composition, biological activity and potential uses. *Adv. Technol.* **2020**, *9*, 54–70. [[CrossRef](#)]
26. United Nations Industrial Development Organization; Handa, S.S.; Khanuja, S.P.S.; Longo, G.; Rakesh, D.D. *Extraction Technologies for Medicinal and Aromatic Plants*; United Nations Industrial Development Organization and the International Centre for Science and High Technology: Trieste, Italy, 2008.
27. Council of Europe. *European Pharmacopoeia 11.2*; European Commission: Strasbourg, France, 2023; Volume 1.
28. Essential Oils: Revised Monograph and New General Chapter in the Ph. Eur. Council of Europe. 16 April 2021. Available online: <https://www.edqm.eu/en/-/essential-oils-revised-monograph-and-new-general-chapter-in-the-ph-eur> (accessed on 14 October 2023).
29. Höß, T. *Alternative Green Extraction Methods for Natural Products*; Universität Regensburg: Regensburg, Germany, 2018.
30. Wang, Y.-H.; Zhang, Y.-R. Variations in compositions and antioxidant activities of essential oils from leaves of Luodian *Blumea balsamifera* from different harvest times in China. *PLoS ONE* **2020**, *15*, e0234661. [[CrossRef](#)] [[PubMed](#)]
31. Baj, T.; Ludwiczuk, A.; Sieniawska, E.; Skalicka-Woźniak, K.; Widelski, J.; Zieba, K.; Główniak, K. GC-MS analysis of essential oils from *Salvia officinalis* L.: Comparison of extraction methods of the volatile components. *Acta Pol. Pharm.* **2013**, *70*, 35–40.
32. Axe, J.; Rubin, J.; Bollinger, T. *The Chemistry of Essential Oils*; Destiny Image Publishers: Shippensburg, PA, USA, 2020; ISBN 0768457025.
33. B Semerdjieva, I.; Shiwakoti, S.; L Cantrell, C.; D Zheljaskov, V.; Astatkie, T.; Schlegel, V.; Radoukova, T. Hydrodistillation Extraction Kinetics Regression Models for Essential Oil Yield and Composition in *Juniperus virginiana*, *J. excelsa*, and *J. sabina*. *Molecules* **2019**, *24*, 986. [[CrossRef](#)]
34. Kusuma, H.S.; Mahfud, M. Comparison of kinetic models of oil extraction from sandalwood by microwave-assisted hydrodistillation. *Int. Food Res. J.* **2017**, *24*, 1697–1702.
35. Gawde, A.; Cantrell, C.L.; Zheljaskov, V.D.; Astatkie, T.; Schlegel, V. Steam distillation extraction kinetics regression models to predict essential oil yield, composition, and bioactivity of chamomile oil. *Ind. Crops Prod.* **2014**, *58*, 61–67. [[CrossRef](#)]
36. Sovová, H.; Aleksovski, S.A. Mathematical model for hydrodistillation of essential oils. *Flavour. Fragr. J.* **2006**, *21*, 881–889. [[CrossRef](#)]
37. Both, S.; Strube, J.; Cravatto, G. Mass Transfer Enhancement for Solid–Liquid Extractions. In *Green Extraction of Natural Products*; Chemat, F., Strube, J., Eds.; Wiley: Hoboken, NJ, USA, 2015; pp. 101–144.
38. Nitsche, M.; Gbadamosi, R. Steam Distillation. In *Practical Column Design Guide*; Nitsche, M., Gbadamosi, R., Eds.; Springer International Publishing: Cham, Switzerland, 2017; pp. 187–213; ISBN 9783319516875.
39. Sixt, M.; Uhlenbrock, L.; Strube, J. Toward a Distinct and Quantitative Validation Method for Predictive Process Modelling—On the Example of Solid-Liquid Extraction Processes of Complex Plant Extracts. *Processes* **2018**, *6*, 66. [[CrossRef](#)]
40. Schmidt, A.; Helgers, H.; Lohmann, L.J.; Vetter, F.; Juckers, A.; Mouellef, M.; Zobel-Roos, S.; Strube, J. Process analytical technology as key-enabler for digital twins in continuous biomanufacturing. *J. Chem. Tech. Biotech.* **2022**, *97*, 2336–2346. [[CrossRef](#)]
41. Uhlenbrock, L. Quality-by-Design zur systematischen Entwicklung von Wertschöpfungsprozessen pflanzlicher Rohstoffe. Ph.D. Thesis, Technische Universität Clausthal, Clausthal-Zellerfeld, Germany, 2021.
42. Jensch, C.; Knierim, L.; Tegtmeier, M.; Strube, J. Development of a General PAT Strategy for Online Monitoring of Complex Mixtures—On the Example of Natural Product Extracts from Bearberry Leaf (*Arctostaphylos uva-ursi*). *Processes* **2021**, *9*, 2129. [[CrossRef](#)]

43. Udugama, I.A.; Lopez, P.C.; Gargalo, C.L.; Li, X.; Bayer, C.; Gernaey, K.V. Digital Twin in biomanufacturing: Challenges and opportunities towards its implementation. *Syst. Microbiol. Biomanuf.* **2021**, *1*, 257–274. [CrossRef]
44. Chen, Y.; Yang, O.; Sampat, C.; Bhalode, P.; Ramachandran, R.; Ierapetritou, M. Digital Twins in Pharmaceutical and Biopharmaceutical Manufacturing: A Literature Review. *Processes* **2020**, *8*, 1088. [CrossRef]
45. García, C.E.; Prett, D.M.; Morari, M. Model predictive control: Theory and practice—A survey. *Automatica* **1989**, *25*, 335–348. [CrossRef]
46. Yu, D.L.; Gomm, J.B.; Williams, D. On-line predictive control of a chemical process using neural network models. *IFAC Proc. Vol.* **1999**, *32*, 4347–4352. [CrossRef]
47. Jelsch, M.; Roggo, Y.; Kleinebudde, P.; Krumme, M. Model predictive control in pharmaceutical continuous manufacturing: A review from a user's perspective. *Eur. J. Pharm. Biopharm.* **2021**, *159*, 137–142. [CrossRef]
48. Rehrl, J.; Kruisz, J.; Sacher, S.; Khinast, J.; Horn, M. Optimized continuous pharmaceutical manufacturing via model-predictive control. *Int. J. Pharm.* **2016**, *510*, 100–115. [CrossRef]
49. Bhaskar, A.; Barros, F.N.; Singh, R. Development and implementation of an advanced model predictive control system into continuous pharmaceutical tablet compaction process. *Int. J. Pharm.* **2017**, *534*, 159–178. [CrossRef]
50. Uhl, A.; Schmidt, A.; Hlawitschka, M.W.; Strube, J. Autonomous Liquid–Liquid Extraction Operation in Biologics Manufacturing with Aid of a Digital Twin including Process Analytical Technology. *Processes* **2023**, *11*, 553. [CrossRef]
51. Singh, R.; Sahay, A.; Karry, K.M.; Muzzio, F.; Ierapetritou, M.; Ramachandran, R. Implementation of an advanced hybrid MPC-PID control system using PAT tools into a direct compaction continuous pharmaceutical tablet manufacturing pilot plant. *Int. J. Pharm.* **2014**, *473*, 38–54. [CrossRef]
52. Ghosal, P.S.; Gupta, A.K. Determination of thermodynamic parameters from Langmuir isotherm constant-revisited. *J. Mol. Liq.* **2017**, *225*, 137–146. [CrossRef]
53. Ramaswamy, H.S.; van de Voort, F.R.; Ghazala, S. An Analysis of TDT and Arrhenius Methods for Handling Process and Kinetic Data. *J. Food Sci.* **1989**, *54*, 1322–1326. [CrossRef]
54. Atkins, P.W.; de Paula, J. *Physikalische Chemie*, 5. Auflage; Wiley-VCH GmbH: Weinheim, Germany, 2020; ISBN 9783527833191.
55. Stephan, P.; Kabelac, S.; Kind, M.; Mewes, D.; Schaber, K.; Wetzel, T. *VDI-Wärmeatlas*; Springer: Berlin/Heidelberg, Germany, 2019; ISBN 978-3-662-52988-1.
56. Plaza, M.; Marina, M.L. Pressurized hot water extraction of bioactives. *TrAC Trends Anal. Chem.* **2023**, *166*, 117201. [CrossRef]
57. Teo, C.C.; Tan, S.N.; Yong, J.W.H.; Hew, C.S.; Ong, E.S. Pressurized hot water extraction (PHWE). *J. Chromatogr. A* **2010**, *1217*, 2484–2494. [CrossRef]
58. Baerns, M.; Behr, A.; Brehm, A.; Gmehling, J.; Hofmann, H.; Onken, U.; Renken, A.; Hinrichsen, K.-O.; Palkovits, R. *Technische Chemie*, 3. Nachdr; Wiley-VCH: Weinheim, Germany, 2012; ISBN 9783527310005.
59. Endress+Hauser Group Services AG. Geführtes Radar/Laufzeitmessverfahren ToF—Levelflex FMP55 | Endress+Hauser. Available online: <https://www.de.endress.com/de/messgeraete-fuer-die-prozesstechnik/fuellstandssensor/Gef%C3%BChrtes-Radar-Levelflex-FMP55?t.tabId=product-overview> (accessed on 8 January 2024).
60. Novikov, K.; Vranek, P.; Kleinova, J.; Šimon, M. Reducing the Costs of Automated Production Systems. *Acta Mech. Slov.* **2019**, *23*, 44–47. [CrossRef]
61. De Spautz, J. Quantifying the benefits of automation. *ISA Trans.* **1994**, *33*, 107–112. [CrossRef]
62. Adler, D.J.; Herkamp, J.A.; Wiesler, J.R.; Williams, S.B. Life cycle cost and benefits of process automation in bulk pharmaceuticals. *ISA Trans.* **1995**, *34*, 133–139. [CrossRef]

Disclaimer/Publisher's Note: The statements, opinions and data contained in all publications are solely those of the individual author(s) and contributor(s) and not of MDPI and/or the editor(s). MDPI and/or the editor(s) disclaim responsibility for any injury to people or property resulting from any ideas, methods, instructions or products referred to in the content.